

The Nernst Effect in Corbino Geometry

A.V. Kavokin^{a,1,2}, B.L. Altshuler^{a,b,1}, S.G. Sharapov^{c,1}, P.S. Grigoryev^{d,1}, and A.A. Varlamov^{e,1}

^aWestlake University, 18 Shilongshan Road, Hangzhou 310024, Zhejiang Province, China; ^bDepartment of Physics, Columbia University, NY, USA; ^cBogolyubov Institute for Theoretical Physics, National Academy of Science of Ukraine, 14-b Metrologichna Street, Kyiv, 03680, Ukraine; ^dSpin Optics Laboratory, St. Petersburg State University, Ulyanovskaya 1, 198504 St. Petersburg, Russia; ^eCNR-SPIN, Viale del Politecnico 1, I-00133, Rome, Italy

This manuscript was compiled on September 4, 2019

We study the manifestation of the Nernst effect in the Corbino disk subjected to the normal external magnetic field and to the radial temperature gradient. The Corbino geometry offers a precious opportunity for the direct measurement of the magnetization currents that are masked by kinetic contributions to the Nernst current in the conventional geometry. The magnetization currents, also referred to as the edge currents, are independent on the conductivity of the sample which is why they can be conveniently described within the thermodynamic approach. They can be related to the Landau thermodynamic potential for an infinite system. We demonstrate that the observable manifestation of this, purely thermodynamic, Nernst effect consists in the strong oscillations of the magnetic field measured in the center of the disk as a function of the external field. The oscillations depend on the temperature difference at the edges of the disk. Dirac fermions and 2D electrons with a parabolic spectrum are characterized by oscillations of different phase and frequency. We predict qualitatively different power dependencies of the magnitude of the Nernst signal on the chemical potential for normal and Dirac carriers.

Nernst effect | Corbino disk | magnetic oscillations

A Corbino disk represents one of the most important experimental designs for studies of transport effects in solids (1). In contrast to the Hall bar geometry (2), in a Corbino disk the Lorentz force induced by a magnetic field normal to the plane of the structure is not compensated by the induced electrostatic force. The Lorentz force gives rise to circular edge currents that can be studied through the magnetization generated by them (3). These currents are usually referred to as magnetization or diamagnetic currents (4). They are governed by the gradient of the magnetisation in a sample and are formally independent of the electric conductivity henceforth. In classical language they arise because of the reflection of carriers circulating on their cyclotron orbits from the inner and the outer edges of the disk (5, 6). In the range of classically strong magnetic fields, the magnetization currents exhibit oscillations with a periodicity governed by the resonances between Fermi and Landau energy levels (7). These oscillations can be studied e.g. by measuring the magnetic field induced by edge currents in the center of the disk.

The Hall effect in the Corbino geometry has been studied both in classical (8) and quantum (9) limits. In contrast, the most important thermomagnetic effect, namely the Nernst effect, remains poorly explored in the disk geometry. The Nernst effect (10) consists in the induction of an electric current by a combined action of the crossed external magnetic field and the temperature gradient. It may be considered as a heat counterpart of the Hall effect. Recently, the giant Nernst or Nernst-Ettingshausen effects have been observed in graphene (11, 12), in pseudogap phase of quasi-two dimensional high temperature superconductors (13–16), in conventional super-

conducting films being in the fluctuation regime (17, 18).

Generally speaking, the Nernst signal consists of two contributions: the kinetic one and the thermodynamic one. The former is governed by the conductivity of the sample and the derivative of chemical potential of the carriers over temperature. The latter is related to the stationary magnetization currents induced by the temperature gradient: $I_N^{th} = c \left(\frac{\partial m_z}{\partial T} \right) \Delta T$ (where $m_z(T)$ is the magnetization per square of the disk). This relation was initially obtained by Obratsov for the Hall bar geometry more than 50 years ago (4). It is worthwhile to mention that this problem has been readdressed in almost every decade (19–24) due to its importance for the quantum Hall effect, Nernst-Ettingshausen effect in fluctuating superconductors, anomalous thermospin effect in the low-buckled Dirac materials, etc. The existence of magnetization currents is crucial for validity of such fundamental properties of thermomagnetic coefficients as the Onsager relations as well as the Third law of thermodynamics (4, 24, 25). Yet, their existence and importance for the Nernst effect often have been neglected (see for instance (26) and discussion in (27)) or even denied (see (28–30)).

The Corbino geometry offers a unique opportunity for the observation of the purely thermodynamic contribution to the Nernst effect generated exclusively by magnetization currents. Indeed, in the regime of classically strong magnetic fields, if the chemical potential of the electron gas in the disk lies between the Landau quantization levels, the electric current does not propagate between the inner and outer edges of the disk, and one can safely neglect the kinetic part of the Nernst response. In the same regime, in the presence of the magnetic field and temperature gradient, the contribution of the edge currents remains significant, so that the total circular current

Significance Statement

The Nernst effect consists in the induction of an electric current by a combined effect of the external magnetic field and the temperature gradient. We consider a Corbino disk geometry, where the temperature difference is applied between the outer and inner edges of the disk, while the magnetic field is perpendicular to the plane of the disk. We show that the circular diamagnetic currents flowing along the edges of the disk are the oscillatory functions of the filling factor of Landau levels of the electron gas in the disk. The Corbino geometry offers a unique opportunity for observation of the magnetization currents that have a purely thermodynamic nature, e.g. are independent of the conductivity of the sample.

¹ All the authors contributed equally to this work and to writing the manuscript.

² E-mail: a.kavokin@westlake.edu.cn

in the sample is dominated by magnetization currents.

Below we calculate the magnetization currents of carriers characterized by parabolic or Dirac energy dispersion relations (31) in a Corbino disk subjected to a radial temperature gradient and a strong magnetic field B applied normally to the plane. Specifically, we analyze the magnetic field B_{ind} induced by these currents in the center of the disk that can be experimentally measured e.g. by a SQUID magnetometer (32, 33). We show that this field experiences pronounced unharmonic oscillations as a function of the external field B . These oscillations are dominated by an interplay of two competing factors. The background contribution to the induced magnetic field that exists at zero temperature gradient is proportional to the second (for normal carriers) or third (for Dirac fermions) power of the chemical potential. At low temperatures, the chemical potential exhibits a characteristic saw-tooth oscillatory dependence on the magnetic field that is well-known (34, 35). The second contribution to the magnetization, proportional to the difference of temperatures at the inner and the outer edges of the disk, is governed by the differential entropy per particle dependence on the external magnetic field (36). It can be calculated knowing the density of electronic states in the system for given temperature and magnetic field (37, 38). The difference of the values of the induced magnetic field B_{ind} measured for the opposite signs of the temperature variation between inner and outer edges of the disk is no more sensitive to the background effect and allows for extracting the contribution induced by the temperature gradient, i.e. the Nernst effect. The shape and the period of Nernst current oscillations in the Corbino geometry carry a precious information on the type of carriers and on the trajectories of topologically protected edge currents. The universal link between the Nernst current and the induced magnetization established in this work offers a powerful tool for the experimental studies of transport phenomena in two-dimensional crystals.

The relation between the edge current and thermodynamic potential in the Corbino geometry

The edge currents in Corbino geometry can be related to the thermodynamic potential of the system basing on very generic thermodynamic consideration. Indeed, let us start from consideration of a homogeneous metallic disk of the radius R , placed in a thermal reservoir of temperature T and subjected to the magnetic field H normal to the plane of the disk. The contribution to the thermodynamic potential dependent on the induced current can be written as

$$\Omega_H = \frac{1}{c} \int \mathbf{j}(\mathbf{r}) \mathbf{A}(r) dV \quad [1]$$

where \mathbf{A} is the vector potential. Consequently, the current can be expressed as

$$\mathbf{j}(\mathbf{r}) = \frac{c}{hS} \left(\frac{\partial \Omega_H}{\partial \mathbf{A}} \right), \quad [2]$$

with $S = \pi R^2$ being the area of the disk and h its height. Assuming that the radius of the disk is much larger than the magnetic length, one can choose the vector potential in the Landau gauge, $\mathbf{A} = (0, Hx)$ that yields for total current flowing through the disk

$$\frac{J}{h} = \frac{c}{hS} \frac{1}{H} \int_0^R \frac{\partial \Omega_H}{\partial x} dx = \frac{c}{HS} \Omega_H(T). \quad [3]$$

From the Fig. 1a one can see that the current is concentrated only in the vicinity of the edge of the disk.

Now one can represent the Corbino disk (ring) as the large disc of the radius R_2 from which a smaller disk of the radius R_1 is cut out. As a result, the total current flowing along the edges is given by the difference between the outer and internal edge currents. Both currents are defined by the same Eq. (3), taken with different areas of the disk. Accounting for the temperature difference between the edges, one can finally obtain

$$J_{\text{tot}} = \frac{c}{H} \left[\frac{\Omega(T_2)}{S_2} - \frac{\Omega(T_1)}{S_1} \right]. \quad [4]$$

The derivation above is based on classical arguments that may seem contradictory to the quantum nature of Landau diamagnetism. This is why, in the following section we will reproduce the final expression for the current (3) in the framework of a quantum mechanical approach.

The microscopic approach to calculation of edge currents

The eigenvalue problem. Let us consider now the Corbino disk with the inner edge radius R_1 and the outer edge radius R_2 subjected to the magnetic field H applied normally to the disk plane in microscopic approach. We are interested here in the regime of classically strong magnetic fields, where the energy separation between the neighbouring Landau levels exceeds their broadening, yet remaining small with respect to the Fermi energy: $\max\{T, \Gamma\} \ll \hbar\omega_c \ll E_F$, where T is temperature, Γ is the Dingle temperature, ω_c is the cyclotron frequency, E_F is the Fermi energy. In what concerns the requirements to the disk geometry, we assume that $R_1, R_2, R_2 - R_1 \gg l_B$, where the magnetic length is $l_B = \sqrt{\hbar c/|e|H}$.

We use here the thermodynamic approach to the Nernst effect developed in Refs. (4, 7). Namely, we describe the system by the Gibbs thermodynamic potential

$$\Omega = -2kT \sum_{\alpha} \ln \left[1 + e^{\frac{\mu - \varepsilon_{\alpha}}{kT}} \right], \quad [5]$$

where ε_{α} are the eigenvalues, and the summation is performed over the complete set of the quantum numbers $\{\alpha\}$, $\mu(T)$ is the chemical potential of the electron gas, coinciding with the Fermi energy at zero temperature. The spin degeneracy of the electron gas under study is postulated, that results in the appearance of the factor 2 in Eq. (5). In the case corresponding to the 2D gas of free electrons (2DEG) subjected to a magnetic field, the electronic Hamiltonian has the familiar Landau form (the specifics of carriers having a Dirac dispersion will be discussed later):

$$\hat{H} = -\frac{\hbar^2}{2m} \frac{d^2}{dx^2} + \frac{m\omega_c^2}{2} (x - x_0)^2 \quad [6]$$

with $\omega_c = |e|H/(mc)$. The set of quantum numbers is $\alpha = \{x_0, n\}$, where $x_0 = l_B^2 k_y$ is the x -coordinate of the center of the electron cyclotron orbit, k_y is the tangential component of the electron momentum (see the schematic in Figure 1a), n is the index of the energy quantization level in the potential induced by the magnetic field (with the minimum at the point x_0).

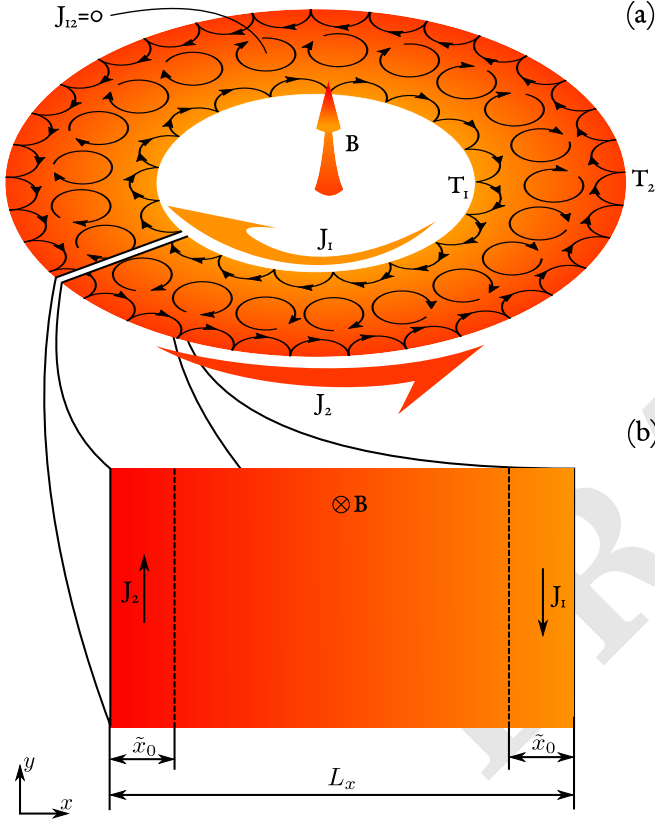


Fig. 1. a). The schematic showing the edge currents flowing in a Corbino disk subjected to an external magnetic field normal to its plane and to a radial temperature gradient. b). The schematic showing the edge currents flowing in a conducting strip subjected to an external magnetic field normal to its plane.

The rule for summation over eigenvalues in Eq. (5) takes a form

$$\sum_{\alpha} \dots = \frac{|e|H L_y}{c 2\pi\hbar} \int_{-\infty}^{\infty} dx_0 \sum_{n=0}^{\infty} \dots, \quad [7]$$

where L_y is the linear dimension of the system along the edge.

The Schrödinger equation with the Hamiltonian (6) and the specific boundary conditions $W_{\alpha}(0) = W_{\alpha}(L_x) = 0$ (Teller's model (5)) determine the spectrum ε_{α} and the set of eigenfunctions:

$$\hat{H}W_{\alpha}(x) = \varepsilon_{\alpha}W_{\alpha}(x). \quad [8]$$

The latter turn out to be the Weber functions $W_{\alpha}(x)$ Ref. (39), while the electron eigenenergies in the vicinity of the edge $x = 0$ can be approximated by:

$$\varepsilon_{\alpha} = \hbar\omega_c \begin{cases} (n + \frac{1}{2}) + \frac{2^n}{\sqrt{\pi n!}} \left(\frac{x_0}{l_B}\right)^{2n+1} \exp\left[-\frac{x_0^2}{l_B^2}\right], & x_0 \gg l_B \\ 2(n + \frac{3}{4}) - 2\frac{(2n+1)\Gamma(n+1/2)}{\pi n!} \left(\frac{x_0}{l_B}\right), & x_0 \lesssim l_B \end{cases} \quad [9]$$

(we note that the similar expressions were obtained in Ref. (6), while some errors in the coefficients and the erroneous factor of “2” in the exponential function are present in that work.) The upper line in (9) corresponds to the cyclotron orbits centered far from the edges ($x_0 \gg l_B$). The energy spectrum for these states coincides with the Landau one with an exponential accuracy. The lower line describes the energy spectrum for the states whose orbits are centered close to the border ($x_0 \lesssim l_B$). The doubling of the cyclotron frequency that appears in the first term is due to the supplementary quantum confinement of carriers in a half-parabolic potential that appears due to their reflection from the boundary.

The edge currents calculated from the first principles. We consider a macroscopic Corbino disk and assume that the curvature of the edges can be safely neglected on the length scale of the cyclotron orbits (see Fig. 1b). In this case, one can calculate the edge currents starting from the exact quantum mechanical expression for the charge flow in a pure quantum state α (6, 40):

$$j_{y\alpha}(x, x_0) = -\frac{|e|\omega_c}{L_y} (x - x_0) W_{\alpha}^2(x). \quad [10]$$

The full current J_{tot} is obtained by summing $j_{y\alpha}$ over all eigenstates $\{\alpha\}$ of the problem, accounting for the occupation numbers $f(\varepsilon_{\alpha}) = [\exp((\varepsilon_{\alpha} - \mu)/kT) + 1]^{-1}$ and integrating over the width of the disk:

$$\begin{aligned} J_{\text{tot}} &= \int_0^{L_x} \sum_{\alpha} j_{y\alpha}(x, x_0) f(\varepsilon_{\alpha}) dx \\ &= -m \frac{|e|\omega_c^2}{\pi\hbar} \sum_{n=0}^{\infty} \int_{-\infty}^{\infty} dx_0 f[\varepsilon_n(x_0), T] \int_0^{L_x} dx (x - x_0) W_{\alpha}^2(x). \end{aligned} \quad [11]$$

One can relate the integral over x in Eq. (11) to the derivative of the eigenenergy over x_0 employing the Feynman theorem (40):

$$\int_0^{L_x} dx (x - x_0) W_{\alpha}^2(x - x_0) = \frac{1}{m\omega_c^2} \frac{\partial \varepsilon_{\alpha}}{\partial x_0}, \quad [12]$$

212 that results in

$$J_{\text{tot}} = -\frac{|e|}{\pi\hbar} \sum_{n=0}^{\infty} \int_{-\infty}^{\infty} \frac{d}{dx_0} \ln \left[1 + \exp \left(\frac{\mu(T) - \varepsilon_n(x_0)}{kT} \right) \right] dx_0. \quad [13]$$

213 We underline that far from the edges of the disk the electron
214 energy levels (9) coincide with the Landau levels with an
215 exponential accuracy, i.e. in this domain $\tilde{x}_0 \lesssim x \lesssim L_x - \tilde{x}_0$
216 the derivative $\partial\varepsilon_\alpha/\partial x_0=0$. The value \tilde{x}_0 can be estimated by
217 imposing the phenomenological requirement(6):
218

$$\left(\frac{\partial\varepsilon_\alpha}{\partial x_0} \right)_{x_0=\tilde{x}_0} = 0.$$

220 One can see from Eq. (9) that $\tilde{x}_0 \sim l_B \sqrt{2n+1}$, which is
221 nothing but the radius of the cyclotron orbit at the n -th
222 Landau level. Having this in mind, the integration in (13)
223 can be restricted to the vicinity of the edges of the sample:
224 $] -\infty, \tilde{x}_0], [L_x - \tilde{x}_0, \infty[$. The contribution to the current from
225 the bulk region tends to zero (see Fig. 1).

226 **The edge currents in an inhomogeneously heated sample.** In
227 order to study the Nernst effect we assume that the inner
228 (outer) edge of the disc is kept at equilibrium with the thermal
229 bath of the temperature T_1 (T_2). We assume that the temper-
230 ature gradient is small enough, so that on the scale of the
231 order of \tilde{x}_0 it can be neglected. In this case the full circular
232 current is determined by the difference of two edge currents:

$$J_{\text{tot}} = J(T_1) - J(T_2), \quad [14]$$

234 where

$$J(T) = -\frac{|e|kT}{\pi\hbar} \sum_{n=0}^{\infty} \ln \left[1 + \exp \left(\frac{\mu(T) - \varepsilon_n(\tilde{x}_0(n))}{kT} \right) \right]. \quad [15]$$

236 Since the sum in (15) is determined by its upper limit one
237 can use the expression for $\varepsilon_n(\tilde{x}_0(n))$ from the upper line of
238 Eq. (9). Neglecting the exponentially small second term, we
239 obtain:

$$J(T) \approx -\frac{|e|kT}{\pi\hbar} \sum_{n=0}^{\infty} \ln \left[1 + \exp \left(\frac{\mu(T) - \hbar\omega_c(n+1/2)}{kT} \right) \right]. \quad [16]$$

241 The Eqs. (14)-(16) describe the total current induced by
242 the external magnetic field in the Corbino geometry. The
243 chemical potential $\mu(B, T, \rho)$ depends on the magnetic field,
244 temperature, and the carrier concentration ρ . Comparing
245 Eq. (16) with the thermodynamic potential calculated for the
246 Landau energy spectrum (see Eqs. (5)-(7))

$$\Omega_L(T) = -2kT \frac{|e|H}{c} \frac{S}{2\pi\hbar} \times \sum_{n=0}^{\infty} \ln \left[1 + \exp \left(\frac{\mu(T) - \hbar\omega_c(n+1/2)}{kT} \right) \right], \quad [17]$$

248 one finds the universal relation which was first derived by
249 Obraztsov in (4):

$$J(T, H, \mu) = \frac{c}{HS} \Omega_L(T, H, \mu). \quad [18]$$

251 Let us stress that the sign in Eq. (18) is the matter of conven-
252 tion: in the chosen form it corresponds the direction of the
253 current flowing along the internal edge of the ring.

254 The problem of calculation of the Gibbs potential in the
255 presence of a homogeneous magnetic field was considered long
256 ago in relation to the de Haas - van Alphen oscillations. The
257 corresponding expression can be easily obtained from (17). In
258 the limit of low temperatures $kT \ll \mu(T)$, the exponential
259 term in the argument of the logarithmic function strongly
260 exceeds unity. The expression for the current thus reduces to

$$J^{2\text{DEG}}(T, \mu) = -\frac{|e|}{\pi\hbar^2} \frac{\mu^2(T)}{2\omega_c}. \quad [19]$$

262 In the case of graphene characterised by the linear dis-
263 persion of Dirac carriers, the Landau quantization leads
264 to the appearance of a non-equidistant energy spectrum
265 ($E_n = \pm\sqrt{2n\hbar}|e|Bv_F^2/c$), in which case the summation in
266 Eq.(15) results in

$$J^{\text{gr}}(T, \mu) = -\frac{c}{H} \frac{|\mu(T)|^3}{3\pi\hbar^2 v_F^2}, \quad [20]$$

268 where v_F is the Fermi velocity.

269 The Nernst oscillations in 2DEG and graphene

270 **Oscillations of the edge currents.** We shall evaluate the sum
271 in (17) applying the Poisson summation formula. This results
272 in the appearance of the oscillating term that is small by a
273 parameter ω_c^2/μ^2 with respect to the principal contributions
274 to each of the edge currents (19) and (20). It is important to
275 note that the chemical potential oscillates as a function of the
276 magnetic field with a magnitude ω_c/μ (7, 31, 35), hence we
277 can restrict ourselves to the consideration of this, principal,
278 contribution, when calculating each of the edge currents. It is
279 important to note, that the sum of two edge currents is zero,
280 if the temperature is constant across the sample. J_{tot} deviates
281 from zero if the radial temperature gradient is introduced
282 as discussed below. On the other hand, the magnetic field
283 induced by two edge currents in the center of the disk is
284 different from zero also in the uniform temperature case. At
285 low temperatures, in a 2D system with a fixed number of
286 particles $\mu(T) = E_F + \tilde{\mu}$, where $\tilde{\mu}$ is the oscillating part of the
287 chemical potential that can be written in the universal form
288 valid both for 2DEG of carriers having a parabolic dispersion
289 and for Dirac fermions in graphene characterised by a linear
290 dispersion:

$$\tilde{\mu} = -\frac{\hbar\omega_c}{\pi} \sum_{l=1}^{\infty} \frac{\psi(l\lambda)}{l} \sin \left[2\pi l \left(\frac{cS(E_F)}{2\pi\hbar B} + \frac{1}{2} + \beta \right) \right] \exp \left(-\frac{2\pi l\Gamma}{\hbar\omega_c} \right), \quad [21]$$

292 where

$$\psi(z) = \frac{z}{\sinh z}, \quad \lambda = \frac{2\pi^2 kT}{\hbar\omega_c} \quad [22]$$

294 is the temperature factor, $S(E_F)$ is the electron cyclotron
295 orbit area in the momentum space, β is the topological part
296 of the Berry phase. In the case of a 2DEG characterized by
297 a parabolic dispersion of charge carriers, $\epsilon = p^2/(2m)$, the
298 electron orbit area is $S(E_F) = 2\pi m E_F$, and the trivial phase,
299 $\beta = 0$. In its turn, for the massless Dirac fermions, $\epsilon = \pm v_F p$,
300 the area is $S(E_F) = \pi E_F^2/v_F^2$, while the cyclotron frequency
301 depends on the Fermi energy $\omega_c = v_F^2|e|H/(c|E_F|)$. In contrast
302 to the case of a 2DEG the phase becomes nontrivial, $\beta = 1/2$.

303 All above is valid for the range of classically strong magnetic
304 fields, $\hbar\omega_c \ll E_F$. (We assume that $E_F > 0$.)

305 Substituting Eq. (21) to Eqs. (19) and (20) one can find
306 explicitly the magnetic field dependence of the edge currents:

$$307 \quad J(T, H) = -\frac{|e| E_F^2}{\pi \hbar^2 \omega_c} \left[\eta + \frac{\tilde{\mu}}{E_F} \right] \quad [23]$$

308 with $\eta = 1/2$ for 2DEG and $\eta = 1/3$ for the Dirac electrons in
309 graphene, respectively.

310 Applying the above expression for the edge currents flowing
311 in the Corbino disk with differently heated inner and outer
312 edges one can find the sum of two edge currents as

$$313 \quad J_{tot}(T_1, T_2) = \frac{|e| E_F}{\pi \hbar^2 \omega_c} [\tilde{\mu}(T_2, H) - \tilde{\mu}(T_1, H)]. \quad [24]$$

314 In the case of a relatively small temperature difference $\Delta T =$
315 $T_1 - T_2 \ll T_1$ one can expand $\tilde{\mu}$ and obtain the explicit
316 dependence of the oscillating total current on the magnetic
317 field:

$$318 \quad J_{tot}(T, \Delta T) = \frac{|e| E_F}{\pi^2 \hbar} \left(\frac{\Delta T}{T} \right) \sum_{l=1}^{\infty} \frac{\psi'(l\lambda)}{l} \\ \times \sin \left[2\pi l \left(\frac{cS(E_F)}{2\pi e \hbar B} + \frac{1}{2} + \beta \right) \right] \exp \left(-\frac{2\pi l \Gamma}{\hbar \omega_c} \right). \quad [25]$$

319 The amplitude factor

$$320 \quad \psi'(l\lambda) = \frac{\lambda l [\lambda \coth(\lambda l) - 1]}{\sinh(\lambda l)} = \begin{cases} \frac{\lambda l}{3} [1 - \frac{7}{30}(\lambda l)^2], & \lambda l \ll 1, \\ 2\lambda l \exp(-\lambda l), & \lambda l \gg 1 \end{cases} \quad [26]$$

321 is presented in Fig. 2 a. In contrast to the conventional factor
322 $\psi(l\lambda)$, it is a nonmonotonic function of temperature. Note
323 that the same function $\psi'(l\lambda)$ appears in the expression for
324 the oscillating part of the Seebeck coefficient in an electron
325 gas subjected to a strong magnetic field (41).

326 The total edge current $J_{tot}(T_1, T_2, \nu)$ as a function of the
327 filling factor of a Landau level

$$328 \quad \nu = \frac{\pi \hbar c \rho}{eB} = \begin{cases} \frac{E_F}{\hbar \omega_c}, & \text{2DEG} \\ \frac{cE_F^2}{\hbar e H v_F^2}, & \text{graphene} \end{cases} \quad [27]$$

329 is plotted in Fig. 2 b. One can see that the period of oscillations
330 for graphene is twice larger due to the valley degeneracy.
331 The phase of oscillations for graphene is shifted with respect
332 to 2DEG. The sharp features correspond to the Fermi level
333 crossing by the Landau levels. Note that the shape of obtained
334 current oscillations shown in Fig. 2 b resembles one of the
335 thermoelectric power coefficient for the 2DEG calculated in
336 (41).

337 **The induced magnetic field and its oscillations in the Corbino**
338 **geometry.** The circular electric currents $J(T_{1,2})$ along the
339 edges of the disk lead to the induction of the magnetic
340 field in the center of the disk $B_{ind}(T_1, T_2) = B_1 + B_2$ with
341 $B_{1,2} = \pm 2\pi J(T_{1,2})/cR_{1,2}$. This field constitutes a diamagnetic
342 response of the ring generated by the persistent currents that
343 have a purely thermodynamic nature

$$344 \quad B_{ind}(T_1, T_2) = \eta \frac{|e| E_F}{\hbar c} \left(\frac{E_F}{\hbar \omega_c} \right) \left(\frac{1}{R_1} - \frac{1}{R_2} \right) + B_{osc}. \quad [28]$$

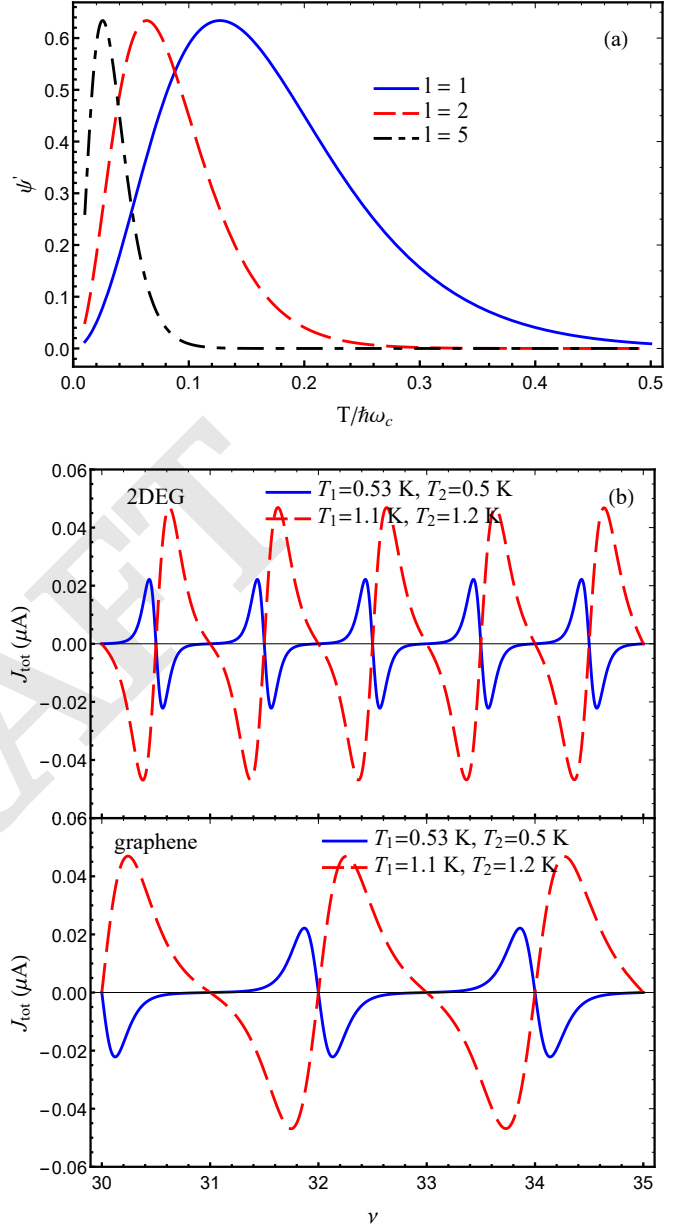


Fig. 2. (a) The dimensionless amplitude factor (26) plotted as a function of temperature T measured in the units of $\hbar\omega_c$ for three different values of l . (b) The sum of two edge currents J_{tot} in μA as a function the Landau filling factor ν that is introduced for the cases of 2DEG and graphene in the body of the paper. The Fermi energy is assumed to be $E_F = 500$ K and the level broadening $\Gamma = 0.5$ K. The cyclotron energy $\hbar\omega_c = E_f/\nu$. Note that $T_1 > T_2$ for the blue curves and $T_1 < T_2$ for the red ones. The direction of the temperature gradient strongly affects the shape of the oscillations.

345 The first term in Eq. (28) monotonously decreases with the
 346 increase of the external magnetic field as a result of the reduction
 347 of the magnitude of the edge currents. The oscillating
 348 part B_{osc} of the induced magnetic field for the specific cases
 349 of carriers with parabolic and linear dispersions is given by

$$B_{osc} = \frac{|e|E_F}{2\pi\hbar c} \sum_{l=1}^{\infty} \frac{1}{l} \left[\frac{\psi[l\lambda(T_1)]}{R_1} - \frac{\psi[l\lambda(T_2)]}{R_2} \right] \\ \times \sin \left[2\pi l \left(\frac{c\mathcal{S}(E_F)}{2\pi e\hbar B} + \frac{1}{2} + \beta \right) \right] \exp \left(-\frac{2\pi l\Gamma}{\hbar\omega_c} \right).$$

351 In order to exclude the background part of B_{ind} that is independent
 352 of the temperature gradient one can study the difference of
 353 the induced fields $\Delta B_{ind}(T_1, T_2) = B_{ind}(T_1, T_2) - B_{ind}(T_2, T_1)$.
 354 The dependence of $\Delta B_{ind}(T_1, T_2)$ on the filling factor is shown
 355 in Fig. 3. The phase and magnitude of the oscillatory features
 356 corresponding to the resonances of Landau and Fermi levels is
 357 strongly dependent on the temperature gradient in the studied
 358 sample. The oscillations depend on the temperature difference
 359 at the edges of the disk. Dirac fermions and 2D electrons with
 360 a parabolic spectrum are characterized by oscillations of different
 361 phase and frequency. We predict qualitatively different
 362 power dependencies of the magnitude of Nernst signal on the
 363 chemical potential for normal and Dirac carriers.

364 Conclusions

365 We have demonstrated that the Corbino geometry offers a
 366 precious opportunity for the observation of the specific Nernst
 367 effect having a purely thermodynamic nature. The effect is
 368 caused by the imbalance of magnetization currents flowing
 369 along the inner and outer edges of the Corbino disk maintained
 370 at different temperatures. We demonstrate that the experimentally
 371 observable manifestation of this thermodynamic Nernst
 372 effect consists in the appearance of the specific oscillations
 373 of the magnetic field measured in the center of the disk as a
 374 function of the external field.

375 We have developed the microscopic model describing such
 376 oscillatory diamagnetic response of the Corbino disk made of
 377 a normal metal and of graphene in the presence of the radial
 378 temperature gradient. The total current exhibits oscillations
 379 corresponding to the resonances of Fermi and Landau levels in
 380 the disk. The value and the direction of the radial temperature
 381 gradient in the sample strongly affect the magnitude and the
 382 shape of the oscillations in the dependence of the induced
 383 magnetic field on the Landau filling factor. An experimental
 384 study of such diamagnetic oscillations in the center of the
 385 Corbino disk would allow for the high precision measurement
 386 of the Nernst effect that is expected to be of strongly different
 387 magnitude in graphene and in normal metals. Such a study
 388 would also shed light on the contribution of the diamagnetic
 389 currents to the Nernst effect that has been a subject of debate
 390 for many years.

391 **ACKNOWLEDGMENTS.** A.A.V. and S.G.Sh. acknowledge the
 392 hospitality of the Westlake University, where this work was started
 393 and mainly accomplished, the support of EC for the RISE Project
 394 CoExAN GA644076. They also are grateful to C. Goupil and
 395 A. Chudnovskiy for illuminating discussion. A.A.V. acknowledges a
 396 support by European Union's Horizon 2020 research and innovation
 397 program under the grant agreement n 731976 (MAGENTA). S.G.Sh.
 398 acknowledges a support by the National Academy of Sciences of

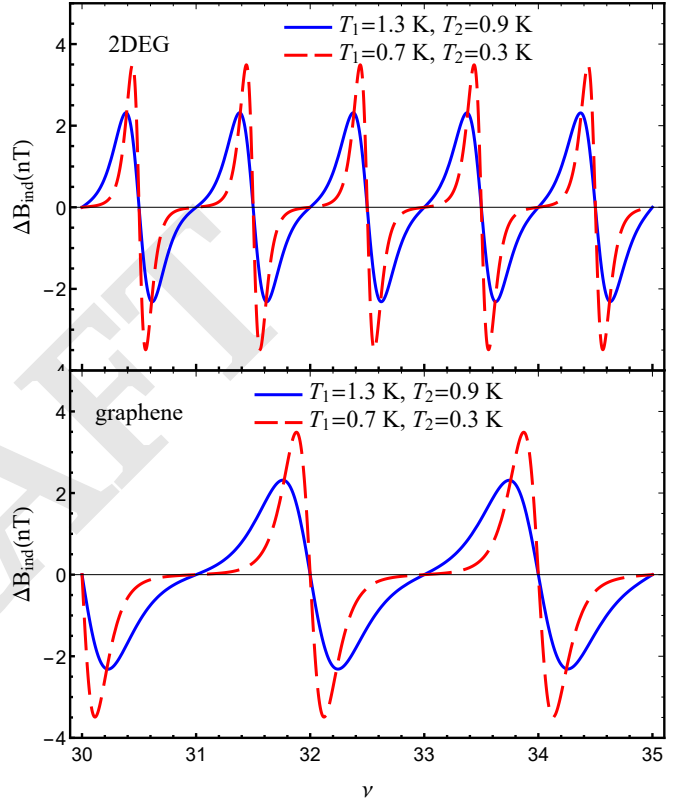


Fig. 3. The contribution to the induced magnetic field ΔB_{ind} at the center of the Corbino disk that is induced by a temperature gradient in nT plotted as a function of the filling factor ν . The upper panel is describing the 2DEG characterised by a parabolic dispersion of charge carriers while the lower panel corresponds to the case of graphene characterised by the linear dispersion of charge carriers. The blue curves are calculated with $T_1 = 1.3K$, $T_2 = 0.9K$ and the red curves correspond to $T_1 = 0.7K$, $T_2 = 0.3K$. The other parameters used in this calculation are $R_1 = 100\mu m$, $R_2 = 110\mu m$, $E_F = 500K$, $\Gamma = 0.5K$.

399 Ukraine (project No. 0117U000236) and by its Program of Fun-
400 damental Research of the Department of Physics and Astronomy
401 (project No. 0117U000240).

402 1. Corbino OM (1911) Azione elettro-magnetica degli ioni dei metalli, deviate dalla traiettoria
403 normale per effetto di un campo magnetico. *Atti accad. nazl. Lincei* 20:342, 416569, 746.
404 2. Janßen M, Veihweger, O, Fastenrath U, Hajdu J (1994) *Introduction to the Theory of the*
405 *Integer Quantum Hall Effect* ed. Hajdu J. (VCH, Weinheim), p. 350.
406 3. Laughlin RB (1981) Quantized hall conductivity in two dimensions. *Phys. Rev. B* 23(10):5632–
407 5633.
408 4. Obraztsov YN (1965) Thermoelectric power of semiconductors in quantizing magnetic fields.
409 *Sov. Phys. Solid State* 7:455.
410 5. Teller E (1931) Der diamagnetismus von freien elektronen. *Zeitschrift für Physik* 67(5):311–
411 319.
412 6. Heuser M, Hajdu J (1974) On diamagnetism and non-dissipative transport. *Zeitschrift für*
413 *Physik* 270(4):289–293.
414 7. Luk'yanchuk IA, Varlamov AA, Kavokin AV (2011) Giant nernst-ettingshausen oscillations in
415 semiclassical strong magnetic fields. *Phys. Rev. Lett.* 107(1):016601.
416 8. Adams EP (1915) The hall and corbino effects. *Proceedings of the American Philosophical*
417 *Society* 54(216):47–51.
418 9. Dolgoplov VT, Shashkin AA, Zhitenev NB, Dorozhkin SI, von Klitzing K (1992) Quantum hall
419 effect in the absence of edge currents. *Phys. Rev. B* 46(19):12560–12567.
420 10. Von Ettingshausen A, Nernst W (1886) Ueber das auftreten electromotorischer krafte in met-
421 allplatten, welche von einem wärmestrome durchflossen werden und sich im magnetischen
422 felde befinden. *Wied. Ann.* 265:343.
423 11. Zuev YM, Chang W, Kim P (2009) Thermoelectric and magnetothermoelectric transport mea-
424 surements of graphene. *Phys. Rev. Lett.* 102(9):096807.
425 12. Checkelsky JG, Ong NP (2009) Thermopower and nernst effect in graphene in a magnetic
426 field. *Phys. Rev. B* 80(8):081413.
427 13. Palstra TTM, Batlogg B, Schneemeyer LF, Waszczak JV (1990) Transport entropy of vortex
428 motion in $\text{YBa}_2\text{Cu}_3\text{O}_7$. *Phys. Rev. Lett.* 64(25):3090–3093.
429 14. Zeh M, et al. (1990) Nernst effect in superconducting y-ba-cu-o. *Phys. Rev. Lett.* 64(26):3195–
430 3198.
431 15. Koshelev A, Logvenov G, Larkin V, Ryazanov V, Soifer K (1991) Observation of magneto-
432 thermoelectric effects in high- t_c superconducting $\text{Tl}_2\text{Ba}_2\text{CaCu}_2\text{O}_x$ single crystals. *Physica*
433 *C: Superconductivity* 177(1):129 – 134.
434 16. Xu ZA, Ong NP, Wang Y, Kakeshita T, Uchida S (2000) Vortex-like excitations and the onset
435 of superconducting phase fluctuation in underdoped $\text{La}_2\text{-xSr}_x\text{CuO}_4$. *Nature* 406(6795):486–
436 488.
437 17. Pourret A, et al. (2006) Observation of the nernst signal generated by fluctuating cooper pairs.
438 *Nature Physics* 2(10):683–686.
439 18. Behnia K, Aubin H (2016) Nernst effect in metals and superconductors: a review of concepts
440 and experiments. *Reports on Progress in Physics* 79(4):046502.
441 19. Smrcka L, Streda P (1977) Transport coefficients in strong magnetic fields. *Journal of Physics*
442 *C: Solid State Physics* 10(12):2153–2161.
443 20. Jonson M, Girvin SM (1984) Thermoelectric effect in a weakly disordered inversion layer
444 subject to a quantizing magnetic field. *Phys. Rev. B* 29(4):1939–1946.
445 21. Oji H, Streda P (1985) Theory of electronic thermal transport: Magnetoquantum corrections
446 to the thermal transport coefficients. *Phys. Rev. B* 31(11):7291–7295.
447 22. Cooper NR, Halperin BI, Ruzin IM (1997) Thermoelectric response of an interacting two-
448 dimensional electron gas in a quantizing magnetic field. *Phys. Rev. B* 55(4):2344–2359.
449 23. Qin T, Niu Q, Shi J (2011) Energy magnetization and the thermal hall effect. *Phys. Rev. Lett.*
450 107(23):236601.
451 24. Gusynin VP, Sharapov SG, Varlamov AA (2014) Anomalous thermospin effect in the low-
452 buckled dirac materials. *Phys. Rev. B* 90(15):155107.
453 25. Serbyn MN, Skvortsov MA, Varlamov AA, Galitski V (2009) Giant nernst effect due to fluctu-
454 ating cooper pairs in superconductors. *Phys. Rev. Lett.* 102(6):067001.
455 26. Ullah S, Dorsey AT (1991) Effect of fluctuations on the transport properties of type-II super-
456 conductors in a magnetic field. *Phys. Rev. B* 44(1):262–273.
457 27. Ussishkin I, Sondhi SL, Huse DA (2002) Gaussian superconducting fluctuations, thermal
458 transport, and the nernst effect. *Phys. Rev. Lett.* 89(28):287001.
459 28. Sergeev A, Reizer MY, Mitin V (2008) Heat current in the magnetic field: Nernst-
460 ettingshausen effect above the superconducting transition. *Phys. Rev. B* 77(6):064501.
461 29. Sergeev A, Reizer M, Mitin V (2010) Thermomagnetic vortex transport: Transport entropy
462 revisited. *EPL (Europhysics Letters)* 92(2):27003.
463 30. Sergeev A, Reizer M, Mitin V (2011) Comment on "giant nernst effect due to fluctuating
464 cooper pairs in superconductors". *Phys. Rev. Lett.* 106(13):139701.
465 31. Sharapov SG, Gusynin VP, Beck H (2004) Magnetic oscillations in planar systems with the
466 dirac-like spectrum of quasiparticle excitations. *Phys. Rev. B* 69(7):075104.
467 32. Barone A, Paterno G (1982) *Physics and Applications of the Josephson Effect*. (Wiley and
468 Son).
469 33. Clarke J, Braginski A, eds. (2004) *The SQUID handbook*. (Wiley-Verlag).
470 34. Shoenberg D (1984) *Magnetic Oscillations in Metals*. (Cambridge University Press, Cam-
471 bridge).
472 35. Champel T, Mineev VP (2001) de Haas -van Alphen effect in two- and quasi-two-dimensional
473 metals and superconductors. *Phil. Mag. B* 81(1):55–74.
474 36. Kuntsevich AY, Tupikov YV, Pudalov VM, Burmistrov IS (2015) Strongly correlated two-
475 dimensional plasma explored from entropy measurements. *Nature Communications* 6(1).
476 37. Varlamov AA, Kavokin AV, Galperin YM (2016) Quantization of entropy in a quasi-two-
477 dimensional electron gas. *Phys. Rev. B* 93(15):155404.
478 38. Galperin YM, et al. (2018) Entropy signatures of topological phase transitions. *Journal of*
479 *Experimental and Theoretical Physics* 127(5):958–983.
480 39. Project BM, Bateman H, Erdélyi A, of Naval Research USO (1953) *Higher Transcendental*
481 *Functions*, Bateman Manuscript Project California Institute of Technology. (McGraw-Hill) No.

v. 2.
40. Landau L, Lifshitz E (2013) *Quantum Mechanics: Non-Relativistic Theory*, Course of theoret-
483 ical physics. (Elsevier Science).
484
41. Pantisulaya A, Varlamov A (1989) Possibility of observation of giant oscillations of thermoelec-
485 tric power in normal metal. *Physics Letters A* 136(6):317–320.
486